17

Mesoscale Wake Clouds in Skylab Photographs

T. Theodore Fujita[a] *and Jaime J. Tecson*[a]

From its vantage point in space, Skylab provided the crewmembers an excellent opportunity for observing and photographing terrestrial objects. During the last manned mission, some unique and remarkable high-resolution photographs were obtained of mesoscale meteorological phenomena. Analyses of selected photographs are contained in this section.

Mesoscale circulations characterized by wake waves and by vortexes are produced in certain limited areas of the world under favorable conditions. Though these circulations do not affect large areas, the phenomena should significantly affect the synoptic conditions of the local areas and possibly influence conditions of nearby regions.

Remarkably enough, Mariner 9 photographs of the atmosphere of Mars show impressive wave-cloud patterns caused by craters that have been identified by Briggs and Leovy (ref. 17-1). Chopra and Hubert (refs. 17-2 and 17-3) have found a quantitative analog to the island patterns in the vortex streets formed behind a solid cylinder comparable in size to the islands. These researchers have found an apparent resemblance between the meteorological mesoscale eddies and the classical vortex street pattern. Formations of cumulus streets and observance of cloud-free paths under winter monsoon situations in certain areas have been described by Tsuchiya and Fujita (ref. 17-4). Investigation of the high-quality photographs detailing the fine structures of mesoscale phenomena that were obtained from Skylab could yield more meaningful evaluations.

[a]The University of Chicago.

WAKE WAVES OF BOUVET ISLAND IN THE SOUTH ATLANTIC

On December 15, 1973, at 14:23 Greenwich mean time (GMT), the Skylab science pilot described "island wake in stratus; 4° W, 48° S; wake toward the east; 150 miles [241 km] long with 20 to 30 crests and valleys under high Sun angle." He obtained a spectacular sequence of three photographs (SL4-137-3631, SL4-137-3632, and SL4-137-3633) that show a pattern of wake waves such as would be expected to be found behind a moving ship. Figure 17-1 is a semirectified photograph of frame SL4-137-3633 and shows the wave pattern developed behind Bouvet Island in the South Atlantic Ocean. Bouvet Island is located at latitude 54°26′ S and longitude 3°24′ E. The elevation of the island is 935 m above sea level. The center of the wake (indicated by the wavy dotted line) may represent a sinusoidal fluctuation of the southwesterly flow against the island. The vertex angle of the wake boundaries is computed to be 38°, which is very close to that of a moving ship.

An unusual feature in the wave pattern is the outward extension of the lateral waves, which commonly is seen only inside the vertex angle of a ship wake. Configurations of this form possibly could occur, however. Stoker (ref. 17-5) indicated that the disturbances or surface waves created by a moving ship are not zero outside the region of the disturbance, but rather they are small and of a different order than within. Thus, in water, the waves normally cannot be detected outside the region of disturbance. In the atmosphere, however, the vertical velocity, though small, is nonzero in this

region. In a saturated layer, therefore, a small vertical velocity may be of sufficient magnitude to produce clouds that would reveal the existence of wave clouds extending beyond the region of disturbance. It is difficult to understand how the wave energy could be transported outward into a large vertex angle of approximately 90°.

The half amplitude of the waves (fig. 17-1) is estimated to be approximately 1 km, which is the island elevation. The wavelength varies between 10 and 15 km, which is one order of magnitude larger than the amplitude. The depth of the atmosphere below the wave is approximately 1 km, indicating that the trough just behind the island might be almost on the ground.

The conclusion drawn from the evidence in figure 17-1 is that the form and occurrence of the atmospheric waves do not correspond to those of deep-water ocean waves, where the kinetic energy of the waves is likely to be lost very quickly. Investigation of the mechanism of wave propagation within and immediately outside the vertex angle behind such an island would be extremely valuable in the study of mesoscale phenomena.

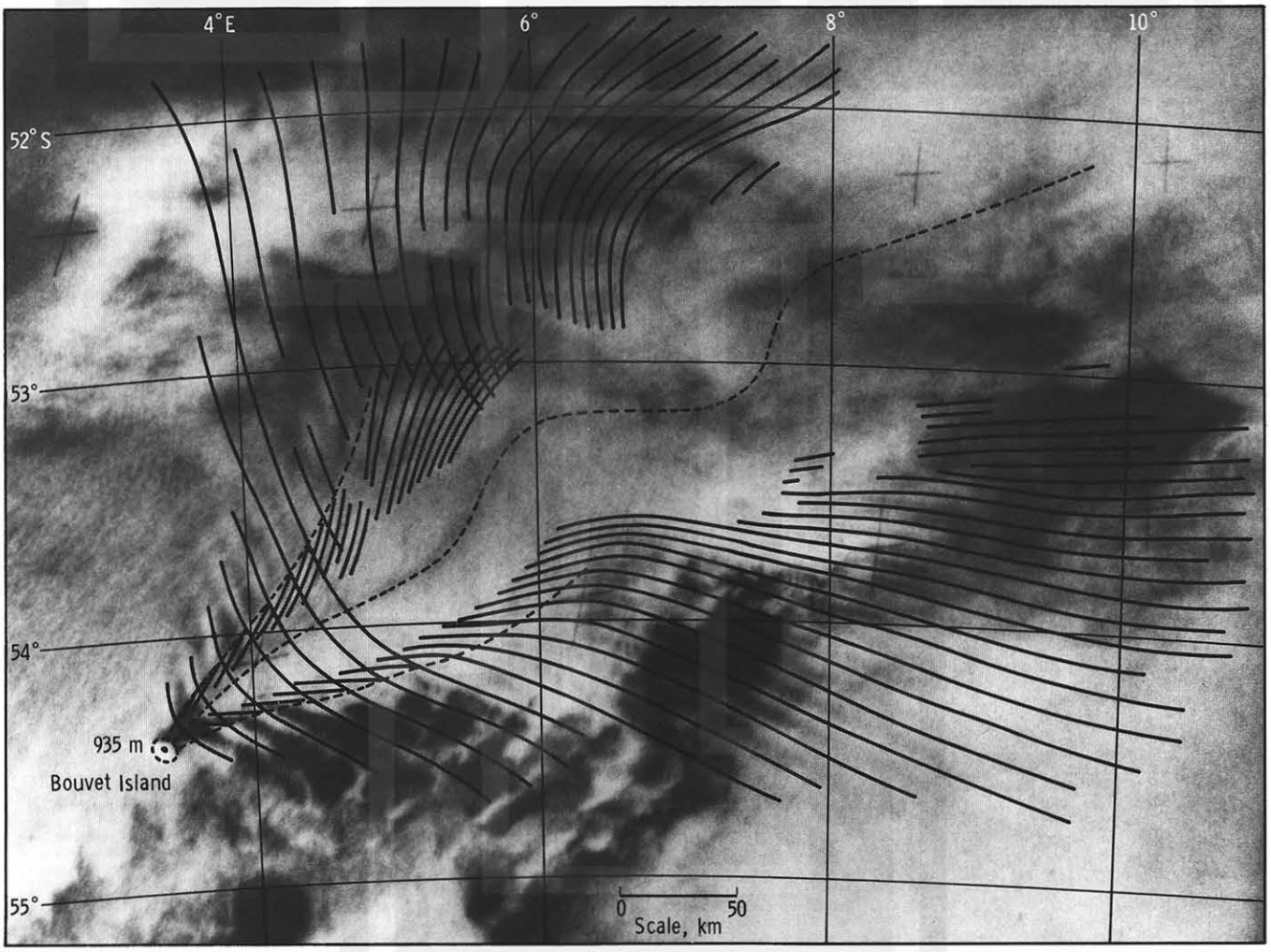

FIGURE 17-1.—Wake waves from Bouvet Island in the South Atlantic; a semirectified photograph taken at 14:23 GMT, December 15, 1973 (SL4-137-3633).

COMPARISON WITH SHIP WAKES

Kelvin's theory (ref. 17-6) of wave patterns created by a moving ship indicates that the V-shaped pattern behind a moving object is similar regardless of the object size as long as the motion is steady along a straight course. When any object, ranging from a duck to a battleship, moves across a water surface, a moving pressure point is created that results in a stationary phase.

The vertical displacement of the water surface at a given point is the integrated effect of the point impulse that moves with an object. When the water is infinite in depth, the point influenced by an object at a specific time moves at the rate of one-half the speed of the object. The instantaneous positions of the influence point are located on a horizontal circle through the ship's position at a specific time. The diameter of the circle coincides with the instantaneous velocity of the ship. The outer boundaries of the V-shaped wake behind the ship are the envelopes of successive circles with increasing diameter in proportion to the distance from the moving ship or obstacle.

The vertex angle is thus expressed by

$$2 \arcsin \frac{1}{3} = 38°56' \qquad (17\text{-}1)$$

which is a constant independent of the object size and speed, as long as the velocity of the object is constant.

Waves caused by a moving pressure point, such as that of a moving ship, are confined to a region of disturbance behind the ship. In particular, two distinct wave sets are apparent in conformity with the fact that each point in the disturbed region corresponds to two influence points. One wave set is arranged roughly at right angles to the course of the ship and designated transverse waves; the other set appears to emanate from the bow of the ship and is called diverging waves. The transverse waves connect the left and right edges of the V-shaped wake. The diverging waves are characterized by the maximum amplitude near the wake boundaries, with amplitudes decreasing to almost zero as they diverge outward.

The wake waves are seen behind moving ships in a lake in figures 17-2 and 17-3. Figure 17-2 is an aerial photograph taken over Lake Michigan, and figure 17-3 was taken over a lake in northern Indiana. Both photographs were taken on July 13, 1974. One of the major differences in the pattern of the wake waves is the existence of the transverse waves in figure 17-2.

Havelock (ref. 17-7) has shown that transverse waves disappear when

$$\frac{c^2}{gh} > 1 \qquad (17\text{-}2)$$

where c is the ship's speed, g is the gravity, and h is the depth. If the depth of Lake Michigan (fig. 17-2) is assumed to be 30 m and $c = 5$ m/sec, the result is

$$\frac{c^2}{gh} = \frac{25}{9.8 \times 30} \cong 0.1 \qquad (17\text{-}3)$$

This number would indicate the existence of transverse waves.

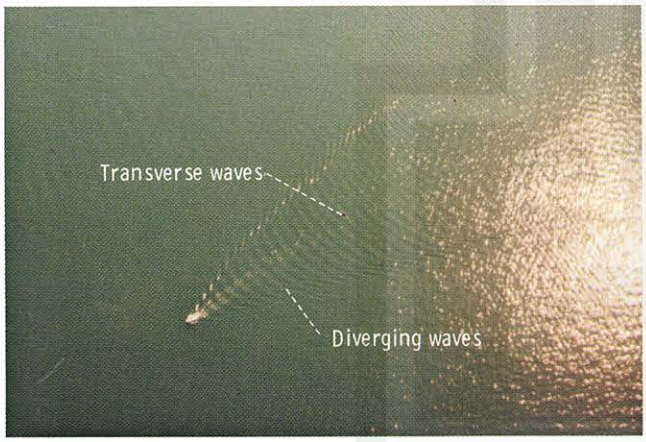

FIGURE 17-2.—Wake waves caused by a slow-moving boat.

FIGURE 17-3.—Wake waves behind a speedboat.

The Indiana lake (fig. 17-3) is very shallow, and the speedboat was moving very fast. If the values $c = 10$ m/sec and $h = 5$ m are used, then

$$\frac{c^2}{gh} = \frac{100}{9.8 \times 5} \cong 2 \qquad (17\text{-}4)$$

which is considerably larger than 1 when the transverse waves are expected to disappear. As seen in figure 17-3, the wake is characterized by diverging waves only.

This discussion on ship wakes suggests that the wave patterns theoretically are applicable to another fluid—the atmosphere—and occur in two forms.

1. Diverging and transverse waves occur when a ship moves slowly on a deep-water surface; they may occur in slow-moving air with a deep layer below the inversion surface.

2. Diverging waves occur alone when a ship moves fast on a shallow-water surface; they may occur in fast-moving air with a shallow layer below the inversion surface.

A law of similarity between ship wakes in the ocean and island wakes in the atmosphere has not been established. This study of imagery shows evidence to promote a law of similarity. The dimensions of islands must be considered in any study because objects of different sizes and shapes cause dissimilar atmospheric

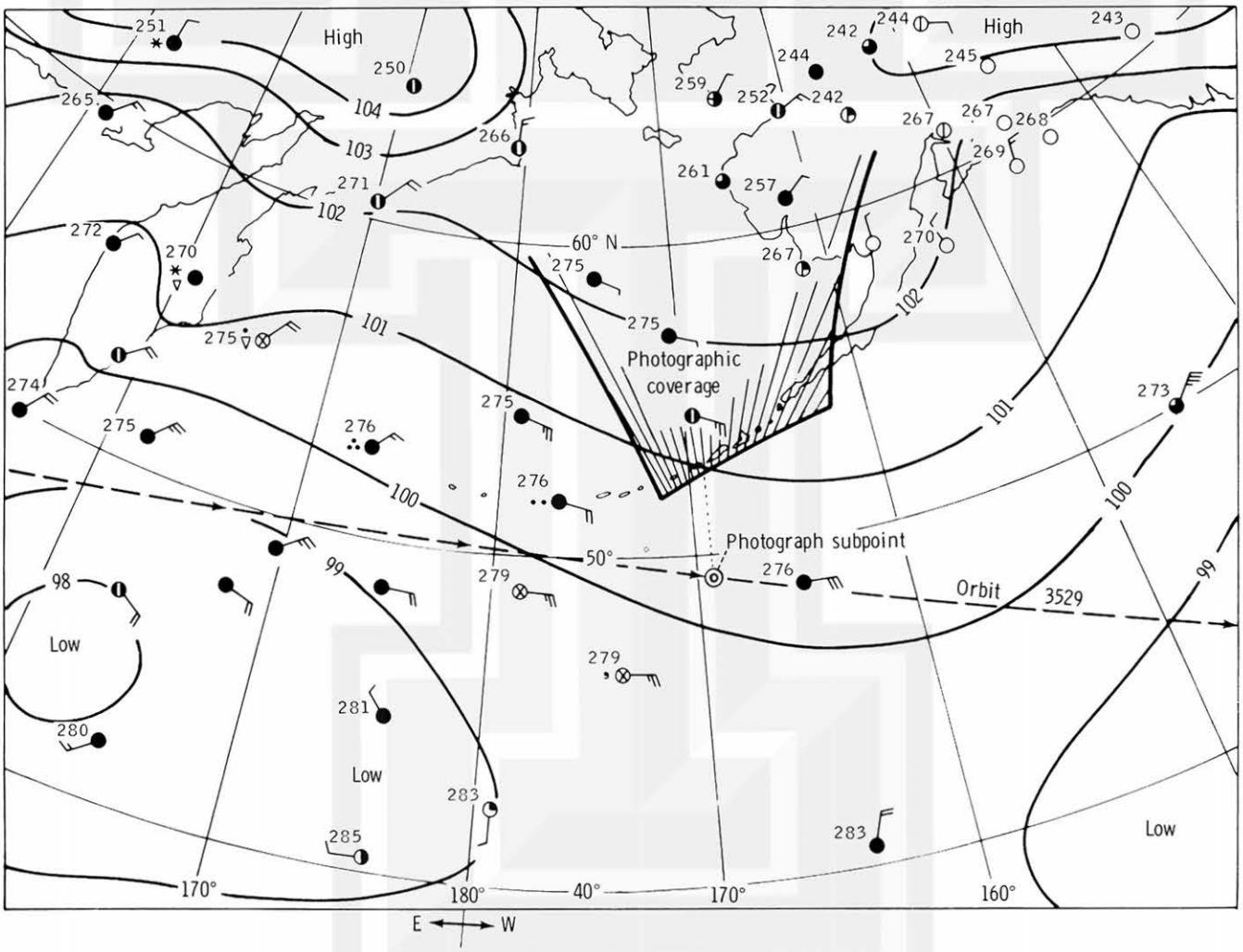

FIGURE 17-4.—The area of the cloud photograph in figure 17-5 superimposed on the surface chart at 00:00 GMT, January 14, 1974. Weather symbols are explained in appendix B.

wakes. For example, the atmospheric wakes downwind from a television tower and from a volcanic island are known to be quite different. Analysis of space photographs must include island size and downwind effects.

WAKE WAVES AND VORTEX STREETS FROM THE ALEUTIAN ISLANDS

On January 14, 1974, the Aleutian Islands were experiencing moderate easterly winds ranging from 10 to 15 m/sec. The upwind side of the island was covered by stratus clouds with tops at approximately 1000 m mean sea level (m.s.l.).

Near the end of orbit 3529, two successive photographs (SL4-140-4111 and SL4-140-4112) of the Aleutian Islands were taken at 01:43 GMT, January 14. Figure 17-4 shows the photograph subpoint, the photographic coverage, and the surface conditions at 00:00 GMT, less than 2 hours before the overflight of Skylab. As seen on the surface map, the flow near the southern tip of the photograph area is uniform: 12 m/sec from the 120° direction.

Under such a uniform flow, atmospheric waves and eddies were created on the lee or downwind side of the islands. Figure 17-5 is a gridded version of the photomosaic of photographs SL4-140-4111 and SL4-140-4112 and covers a 700-km segment of the Aleutian Island chain extending from Amukta Island to Unimak Island.

In figure 17-5, Kármán vortexes are seen to occur predominantly in the wake of large orographic features such as Mount Vsevidof (Umnak), Okmok Crater, Makushin Volcano (Unalaska), and Pogromni Volcano (Unimak). The largest eddy produced in this island chain (marked "P" in fig. 17-5) was formed downwind from the Pavlof Volcano on Pavlof Island (not shown). Wake waves, mostly diverging waves, are found behind small islands and are indicated by solid lines in figure 17-5. Because the characteristics of the flow are uniform, the major factors in producing waves and vortexes are suspected to be the dimensions of the obstacles and velocity of the flow.

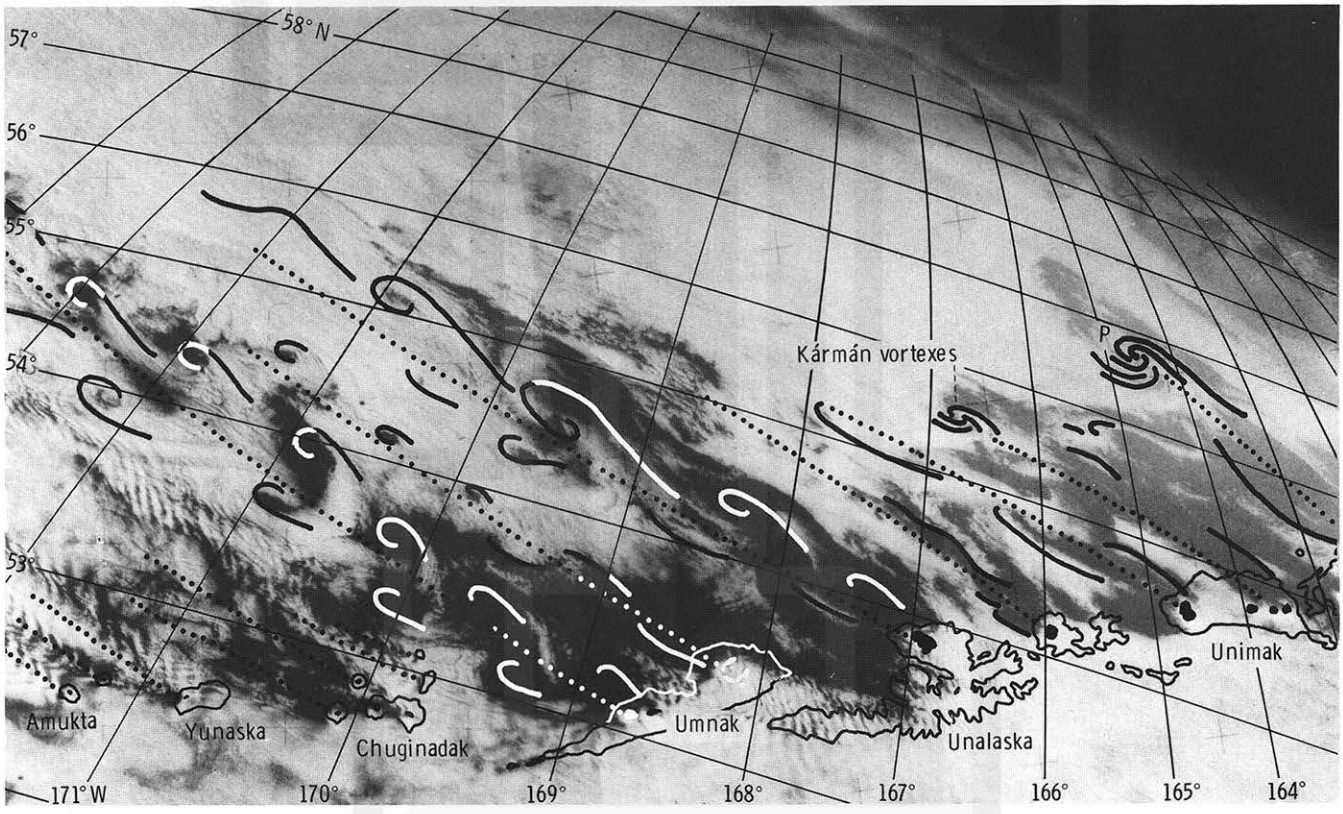

FIGURE 17-5.—Kármán vortex streets and island wakes from the Aleutian Islands at 01:43 GMT, January 14, 1974. Islands are outlined; areas above 1000-m elevation are solid (composite of SL4-140-4111 and -4112).

Figure 17-6 was constructed by rectifying frame SL4-140-4111 into a 1:1 000 000 scale. It should be noted that small peaks are generating a long wake with diverging waves. Analyses of the photographs in figures 17-5 and 17-6 produced a table of wake characteristics (table 17-I). The width of the obstacles in table 17-I is defined as being the cross-sectional dimension at the 300-m elevation m.s.l. As shown in table 17-I, the critical dimension of the obstacle between the wave and eddy formation is 5 km. If an obstacle is 5 km wide or smaller, diverging waves form in the island wake. The height of the obstacle does not influence the wake characteristics as long as the obstacle extends above the top of the stable layers.

According to laboratory estimates on vortex streets, the Reynolds number Re for the lower limit for stable vortex formation is 35. The kinematic eddy viscosity ν corresponding to the critical diameter of the orographic obstacle can be computed from

$$\nu = \frac{DU}{Re} = 2.4 \times 10^7 \text{ cm}^2/\text{sec} \qquad (17\text{-}5)$$

where $D = 5000$ m and the geostrophic wind $U = 17$ m/sec. This value conforms with that estimated by Chopra and Hubert (ref. 17-2).

FIGURE 17-6.—Semirectification showing long wakes with diverging waves. Height contours are 500, 1000, and 1500 m m.s.l. (SL4-140-4111).

TABLE 17-I.— *Wake Characteristics of Aleutian Islands on January 14, 1974*

Obstacle	*Longitude*	*Height, m*	*Width, km*	*Wake type*
Amukta Volcano	171°15′	1056	4	Diverging waves
Chagulak Island	171°09′	1143	2	Diverging waves
Yunaska Island	170°48′	951	5	Diverging waves
Yunaska Island	170°39′	600	4	Diverging waves
Herbert Island	170°07′	1288	5	Waves and eddies
Carlisle Island	170°04′	1610	5	Waves and eddies
Mount Cleveland	169°57′	1730	5	Eddies
Chuginadak Island	169°46′	1170	8	Waves and eddies
Uliaga Island	169°46′	888	2	Diverging waves
Kagamil Island	169°43′	893	2	Diverging waves
Mount Vsevidof	168°31′	1984	24	Vortex street
Mount Vsevidof	168°42′	2109	24	Vortex street
A small peak	168°18′	610	5	Diverging waves
Tulik Volcano	168°08′	1253	22	Vortex street
Makushin Volcano	166°56′	2036	32	Vortex street
Akutan Island	166°00′	1303	12	Vortex street
Pogromni Volcano	164°42′	2002	19	Vortex street

KÁRMÁN VORTEX STREETS FROM KURIL ISLANDS

A photograph obtained at 00:00 GMT on June 4, 1973, shows that vortex streets under a very weak flow condition developed in the wake of the Kuril Islands. The vortex patterns are shown in the semirectified photograph (fig. 17-7). Of interest is the change in the flow direction within a short distance along the island chain. The weather report from Tōkyō, Japan, indicates that Urup Island at 00:00 GMT was 274 K with 1-m/sec wind velocity from 320°. The large-scale flow as estimated from the wake vortex pattern is anticyclonic with a southerly flow between Iturup and Urup Islands. A small cyclonic eddy is seen northeast of Iturup. The northern coast of Iturup is clear, which indicates a southerly flow there.

The cyclonic eddy to the northeast of Urup suggests the existence of a southwesterly flow along the southeastern coast of the island. Off the southwestern tip of Simushir, a weak northwesterly flow is present. A similar flow prevails across the islands of Ketoy, Rasshua, and Matua.

The sea-surface temperature in June around Matua Island is known to be the coldest in the Kuril chain. Almost every day, low stratus and fog cover the area; this condition indicates the existence of a semipermanent inversion layer. The stratification is therefore favorable for the development of vortex streets behind the island. It is unusual, however, to observe the significant change in the flow patterns shown in figure 17-7.

BLOCKING OF EVAPORATION CUMULI BY THE ALEUTIAN ISLANDS

Cumulus streets form when dry, cold air of polar-continental origin passes over an ocean. During this process, heat and moisture are transported from the ocean surface to the atmosphere. When the rate of transportation is very fast, the initial formation of cumuli occurs only a few kilometers offshore. Numerous examples of cumulus streets over the Great Lakes, off the coast of Siberia near the Sea of Japan, and off the Atlantic coast of the United States are visible in Skylab photographs.

One of the most striking photographs of such evaporation cumuli was taken at 01:06 GMT on January 17, 1974, looking north toward the Alaska Peninsula (fig. 17-8). As shown in figure 17-9, the center of a well-developed cyclone with a central pressure of 96.5 kPa was located in the Gulf of Alaska. The air temperature at Fort Yukon was 233 K. A strong surge of cold air is seen in the northwestern sector of the cyclone. The windspeed along the Alaskan coast was approximately 10 m/sec from the north.

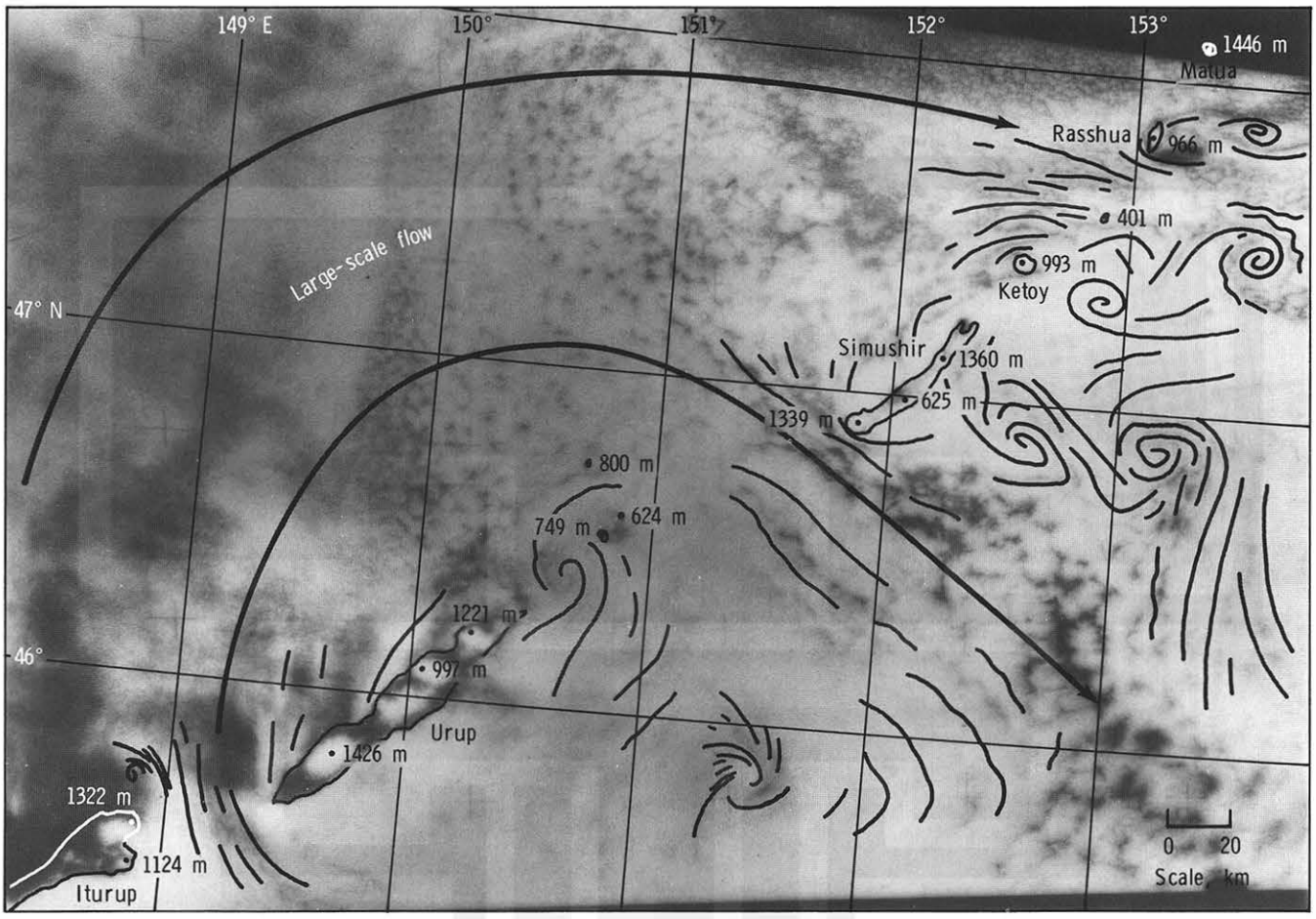

FIGURE 17-7.—Semirectified photograph showing Kármán vortex streets from the Kuril Islands (SL2-5-432).

Figure 17-8 is a gridded photograph that reveals a very narrow cloud-free area along the coast of Kuskokwim Bay, Etolin Strait, and Hazen Bay. The cloud-free path of the cold-air outflow is only several kilometers wide. After the formation of evaporation cumuli, cloud streets develop in the direction parallel to the flow. Numerous streets are seen to extend from the formation points across the Bering Sea toward the Alaska Peninsula. The blocking of these cumulus streets by mountains in the peninsula is similar to a phenomenon frequently seen over Japan under the winter monsoon. However, this phenomenon does not occur in the Atlantic Ocean off the eastern coast of the United States where no blocking mountains exist.

The cloud streets south of the peninsula originate in gaps or low topographic areas where leakage of moisture from the Bering Sea occurs. A most significant feature in figure 17-8 is the cloud-free dark spot south of Mount Veniaminof, a 2560-m peak. A small eddy street extends downwind from the peak region. Another dark spot is found in the wake of Pavlof Volcano, a 2718-m peak. Coastlines are visible within these dark spots that are cloud free, being dominated by strong downslope winds. Neither waves nor vortexes are present in the wake regions of the Alaska Peninsula. The high peaks in the peninsula block the cumulus streets forming over the Bering Sea. One reason for the absence of waves and vortexes within the obstacle wake on the peninsula appears to be the temperature lapse rate of the air just above the sea surface. If the lapse rate is adiabatic or almost adiabatic, the vertical mixing is stimulated by the eddy transport. Such a mixing process will effectively damp both waves and eddies and thus restrict their transport downwind inside the wake regions.

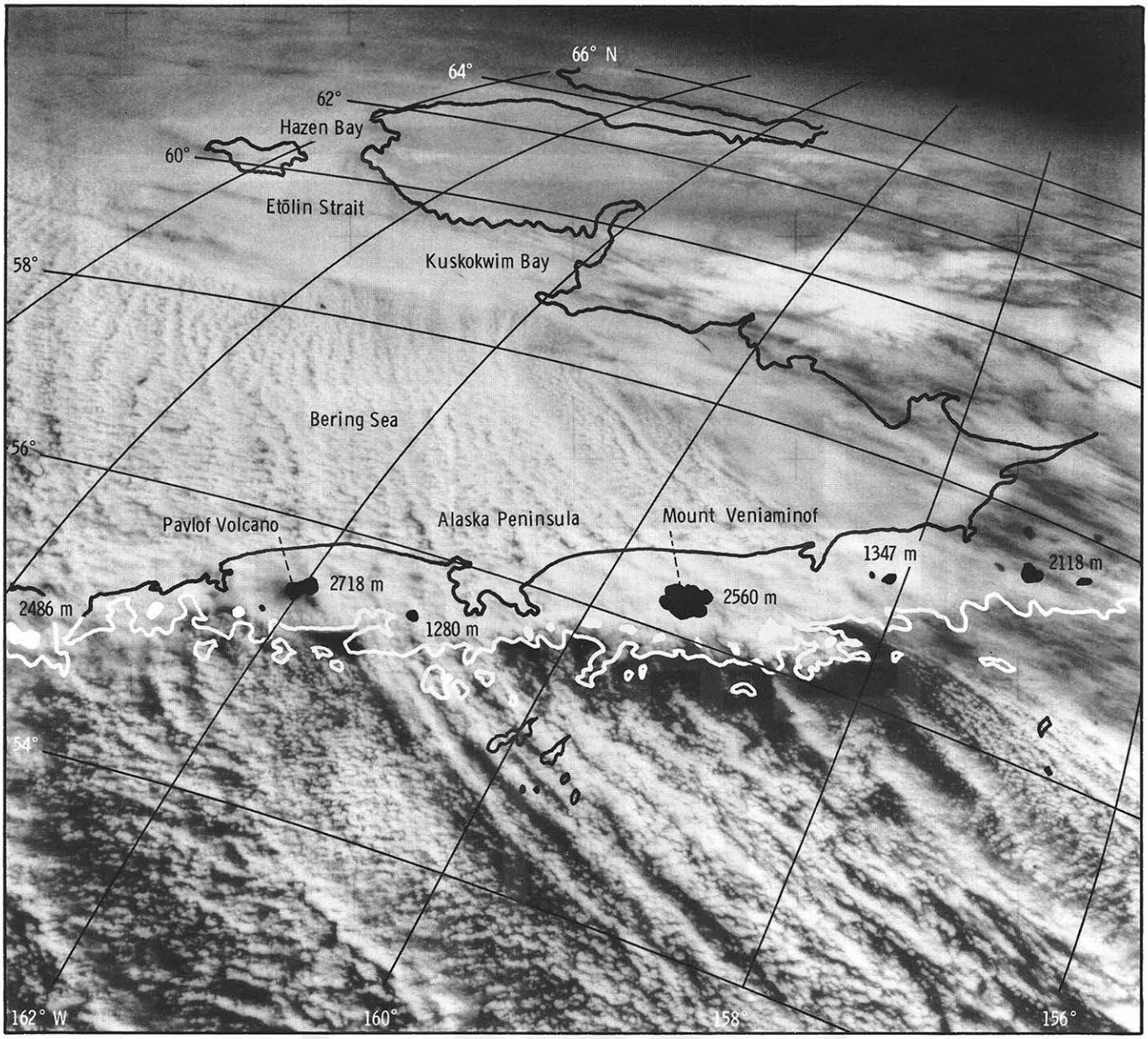

FIGURE 17-8.—Blocking of evaporation cumulus streets by the Aleutian Islands. Grid lines and landmarks placed on photograph taken at 01:06 GMT, January 17, 1974 (SL4-140-4210).

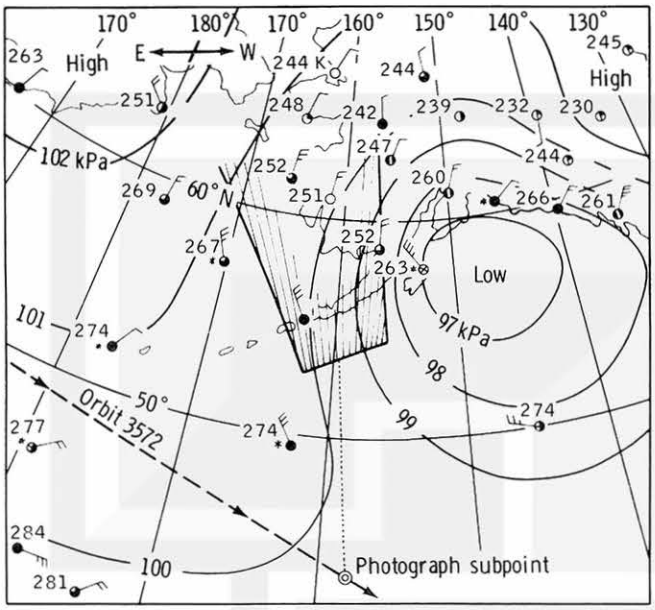

FIGURE 17-9.—Surface map for 00:00 GMT, January 17, 1974, corresponding to the time of figure 17-8. Weather symbols are explained in appendix B.

THERMAL AND MECHANICAL EFFECTS OF SOUTH PACIFIC ISLANDS

During Skylab orbit 3211 on December 23, 1973, an interesting sequence of five photographs (SL4-137-3701 through SL4-137-3705) was taken over the southern end of New Zealand looking toward the south and southeast. Figure 17-10 shows the subpoints and the principal view direction for each photograph and a surface map of the New Zealand area at 00:00 GMT on December 23. The first two photographs were views looking toward the Auckland and Campbell Island areas. Frames 3703 and 3704 show beautiful wake waves extending downwind from Campbell Island. The last photograph shows several cumulus streets or cloud lines forming downwind of Chatham Island.

The cumulus streets that originate over Chatham and Pitt Islands are shown in figure 17-11. The largest street, extending from the northern part of Chatham, originates on the coastline. Because a cloud line often originates over a flat plane downwind from a pointed cape or peninsula, the point of origin of the cloud line could be within the pointed peninsula. Another cloud line originates within the peninsula that extends into Te Whanga Lagoon, the largest lagoon on Chatham Island. Five cloud lines extend southwestward from high spots of southern Chatham. As the cloud line leaves the source, its direction changes to the southwest, which may mean that the direction changed to that of the gradient wind outside the influence of the island.

Cloud lines from Pitt Island are very important because of their appearance. With the exception of the central line originating from the 296-m peak, the cloud lines take the shape of diverging waves. The microscale pattern of the lines implies that they consist of small cumulus cells. However, the island-scale pattern of the plumes shows a configuration of three diverging waves. Further examination of this photograph would be necessary for a better understanding of the transition between cloud lines and waves.

A small cloud line originates from a spot where no island is shown on the map of the South Pacific region (fig. 17-11). The spot might correspond to an area in which the sea-surface temperature is higher and triggers a conditionally unstable atmosphere. Figure 17-12 shows a vertical profile of air temperature and dewpoint temperature from Chatham Island. The layer from the ocean surface to 1.5 km defines the airspace for cloud development; this layer is conditionally unstable and orographic lift or additional heating would result in cumuliform cloudiness. The plume clouds in figure

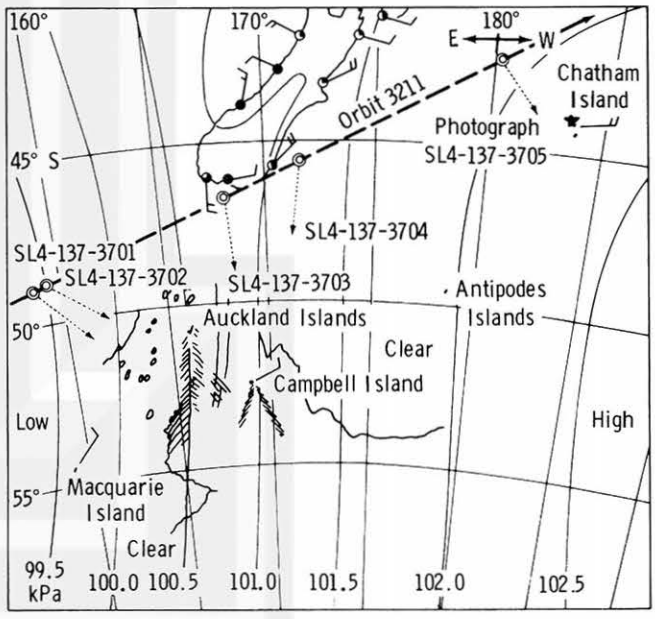

FIGURE 17-10.—Surface map for 00:00 GMT, December 23, 1973. (SL4-137-3701 through SL4-137-3705 were taken at locations of double circles.) Weather symbols are explained in appendix B.

17-11 are embedded in this layer. The stable dry layer between 1.5 and 3 km suppresses cloud development.

An attempt was made to rectify frame SL4-137-3703 for detailed examination of the wake waves from Campbell Island (fig. 17-13). There are two dominant peaks on the island, resulting in the two sources of wake waves in the atmosphere. A minor wake extends from the 465-m peak near the western end of the island. The major wake is originated by the highest (569 m) peak of the island. The combined wake is rather complicated where two sets of waves intersect at acute angles. Unfortunately, no temperature sounding of Campbell Island is available within several hours of the time the photograph was taken.

Winds aloft from Campbell Island show the existence of a significant shear (change in direction and velocity) layer between 1.7 and 2.0 km (fig. 17-14). The advection line of the wake extending toward the 190° direction from the 569-m peak coincides with the flow direction of the lower layer below the shear layer. This may mean that the advection line is the trajectory of the air modified by the island. The center line of the wake obtained by bisecting the V-shaped wake is oriented from the direction 350° to 170°. This orientation is almost the same as the mean value of the windflow direction of the lower layer (10° to 190°) and the upper layer (330° to 150°). These figures indicate that the wake waves propagate with the mean flow of the upper and lower layers.

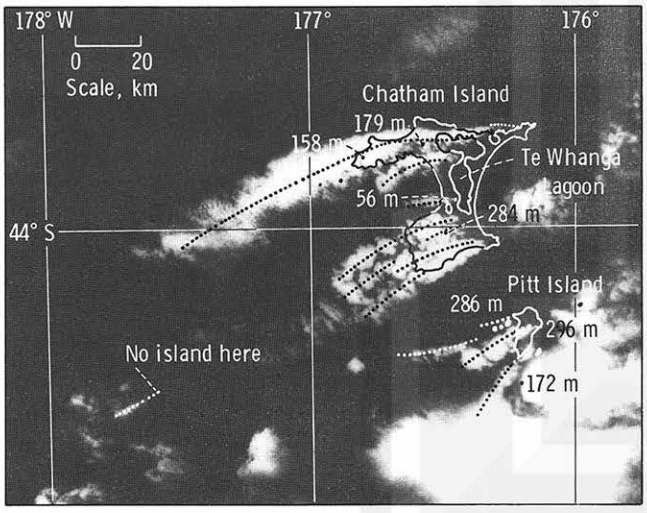

FIGURE 17-11.—Rectified photograph of cumulus streets from Chatham Island taken at 01:14 GMT, December 23, 1973 (SL4-137-3705).

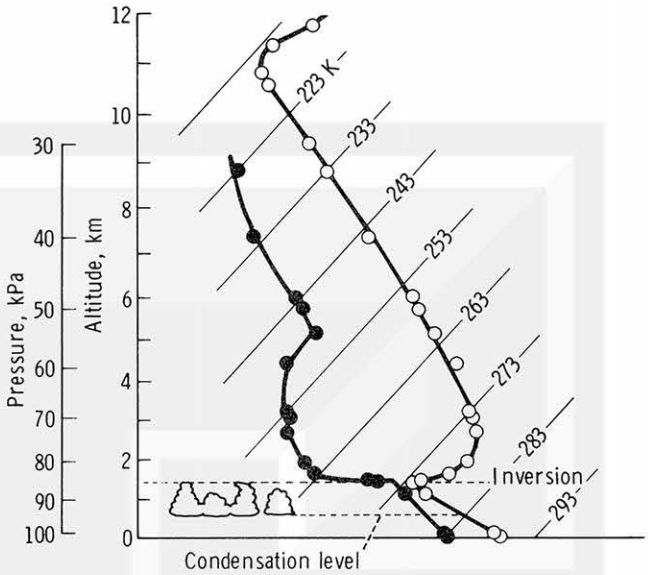

FIGURE 17-12.—Sounding at Chatham Island made at 00:00 GMT, December 23, 1973, 1 hour 14 minutes before figure 17-11 was taken.

DRY AND WET WAKES FROM ANTIPODES ISLANDS

A significant change in the wake of the Antipodes Islands occurred between December 16 and 17, 1973, and was revealed in two Skylab photographs taken 23 hours apart. The photograph taken at 01:13 GMT on December 16 (fig. 17-15) shows small patches of clouds on top of high peaks on the Antipodes Islands southeast of New Zealand. Although a distinct pattern of atmospheric wake waves is visible in figure 17-15, these waves are not characterized by clouds. If cumuliform clouds are embedded inside the waves, their brightness cannot be as low as shown on the photograph.

The authors suspect that the waves were made visible by the differential depth of pollutants trapped beneath the temperature inversion layer. More pollutants are found beneath the crests, whereas fewer pollutants will exist beneath the troughs. Such waves may be identified as "dry waves." Conversely, wake waves with condensed water droplets or clouds may be called "wet waves."

Figure 17-16 is the photograph taken at 00:20 GMT on December 17, 23 hours 07 minutes after figure 17-15 was taken. Significant "wet waves" are seen behind the same island. A considerable change in the flow direction also has occurred.

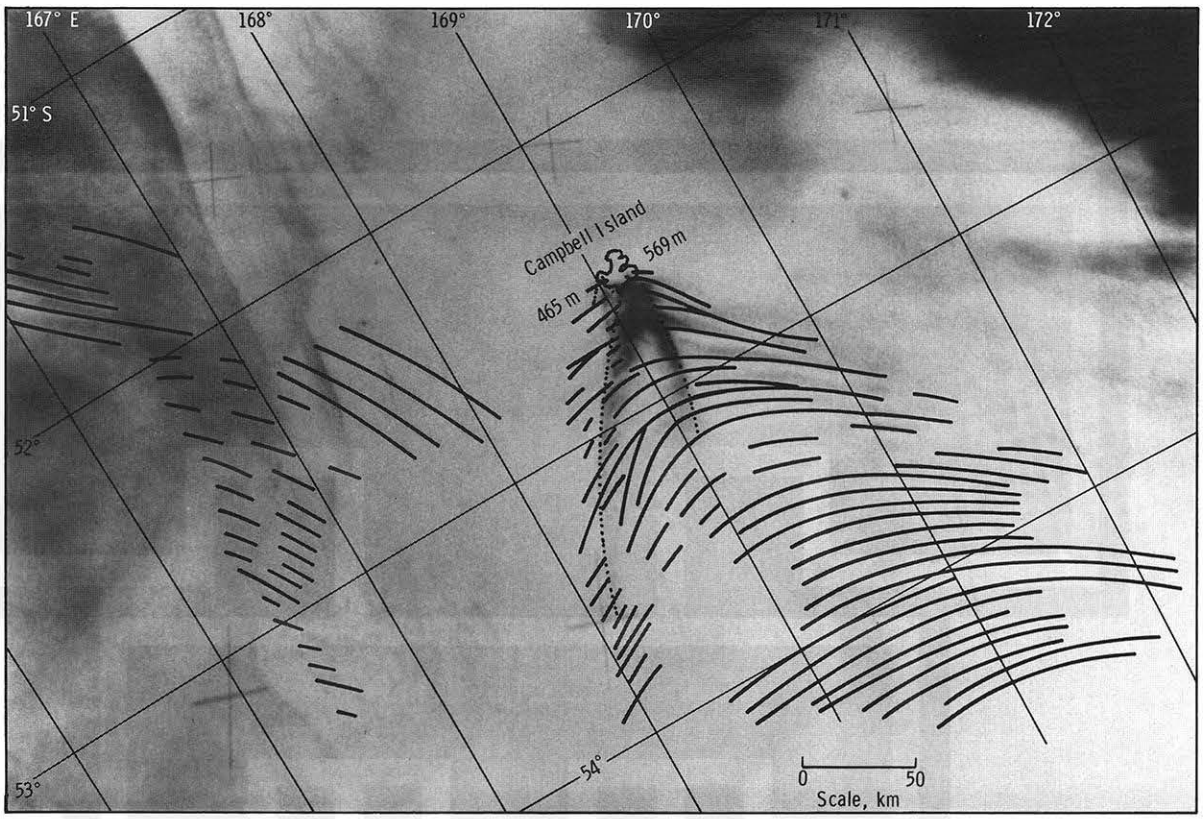

FIGURE 17-13.—Wake waves from Campbell and Auckland Islands south of New Zealand photographed at 01:11 GMT, December 23, 1973 (enlargement of SL4-137-3703).

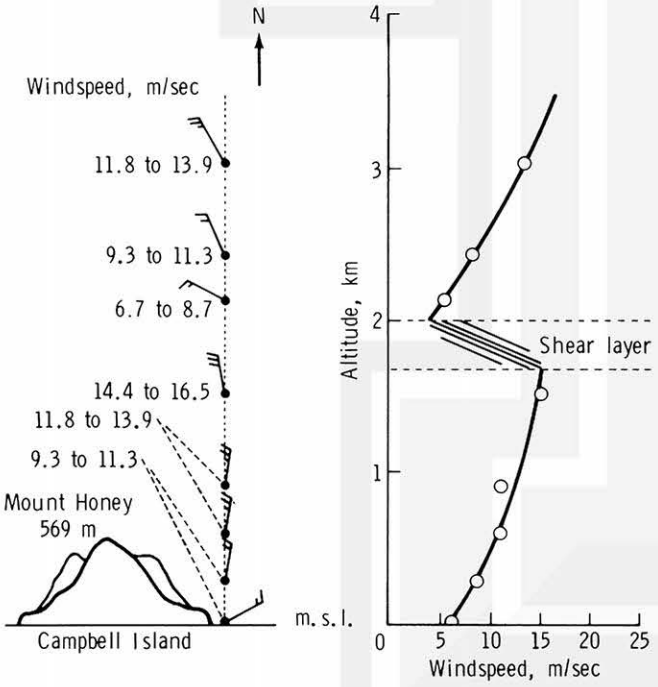

FIGURE 17-14.—Vertical distribution of winds over Campbell Island at 00:00 GMT, December 23, 1973. Weather symbols are explained in appendix B.

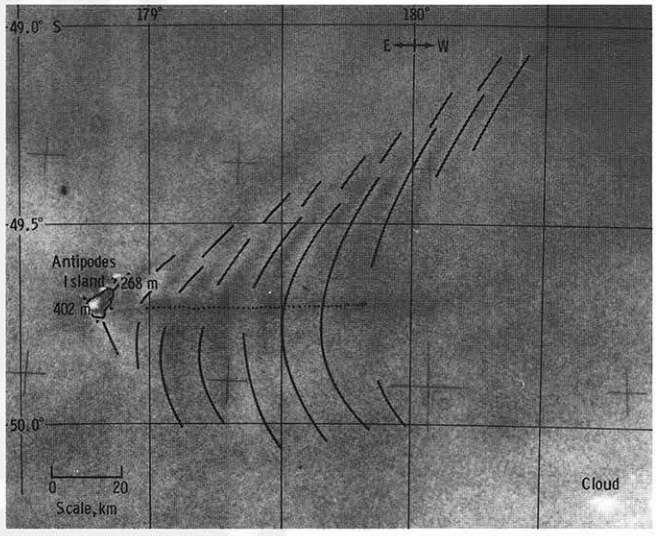

FIGURE 17-15.—Wake waves behind the Antipodes Islands made visible by the differential thickness of air pollution. Dry wakes without clouds are seen in this rectified photograph taken at 01:13 GMT, December 16, 1973 (SL4-137-3655).

FIGURE 17-16.—Wake waves behind the Antipodes Islands made visible by wave clouds. This photograph of wet wakes with clouds was taken at 00:20 GMT, December 17, 1973 (SL4-137-3668).

The difference in the surface weather maps within 24 hours is shown in figure 17-17. A major change appears to be the advancement of a cyclone toward the east-northeast. The flow direction at the location of the Antipodes Islands shifted from westerly to northerly. Meanwhile, clouds of several types moved into the area. The surface weather maps also indicate that New Zealand was the likely source of the pollution that made wakes in the area of Antipodes (fig. 17-15) easy to see.

A vertical profile of the air temperature, dewpoint temperature, and windspeed as recorded on Campbell Island December 16, 1973, is given in figure 17-18. The vertical temperature structure indicates the lowest cloud tops at 1 km and a few clouds at 2 km and at 5 km. The isothermal layer from 0.5 to 2.5 km is a mark of low-level stability.

If the characteristics of the stratification at Campbell Island are applied to the Antipodes Islands, the temperature lapse rate is favorable for the atmospheric wave propagation. Such a stable lapse rate will minimize the kinetic energy dissipation through eddy transport of low-level momentum.

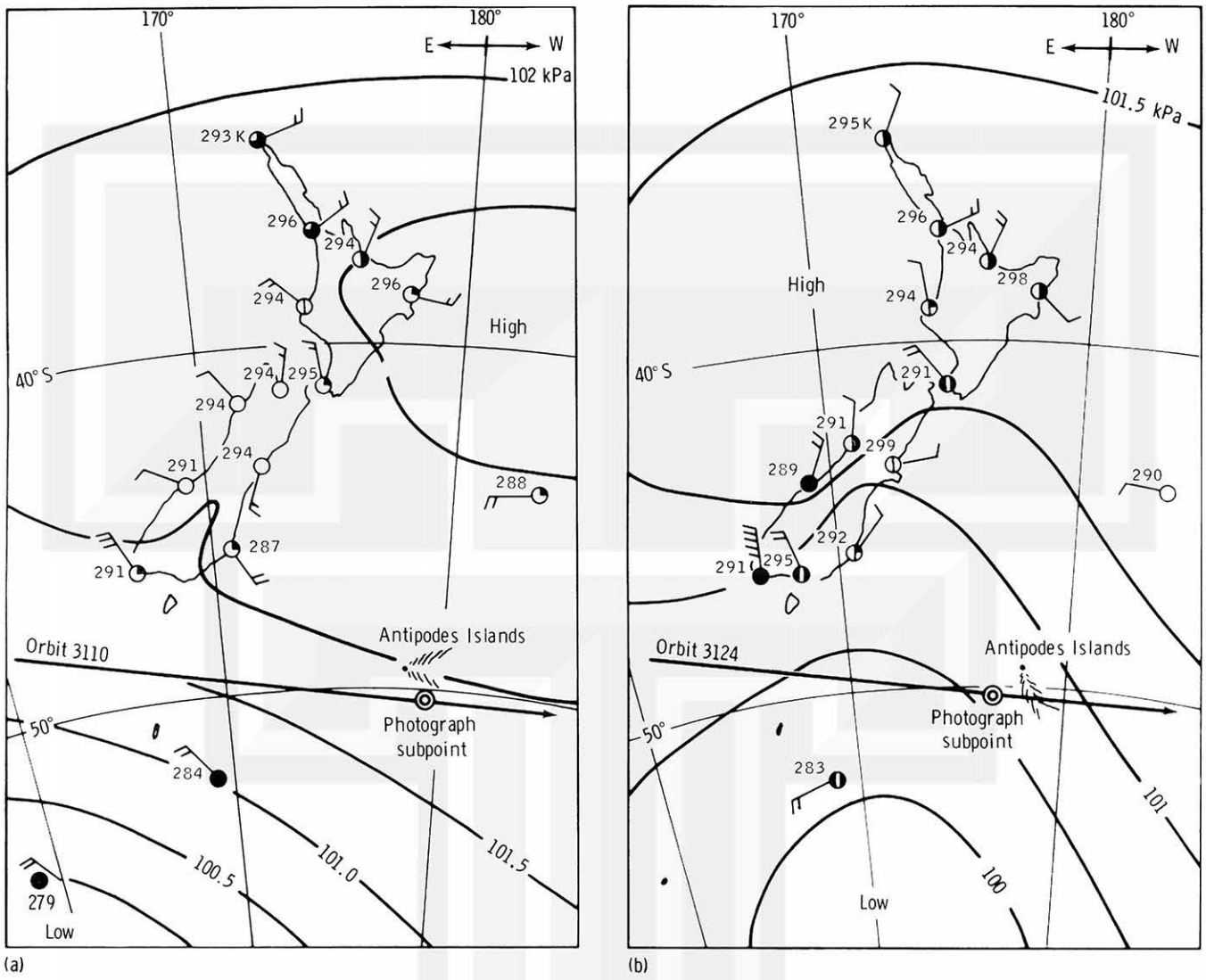

FIGURE 17-17.—Change in the surface flow during the 24-hour period from December 16 to December 17, 1973. Weather symbols are explained in appendix B. (a) 00:00 GMT, December 16. (b) 00:00 GMT, December 17.

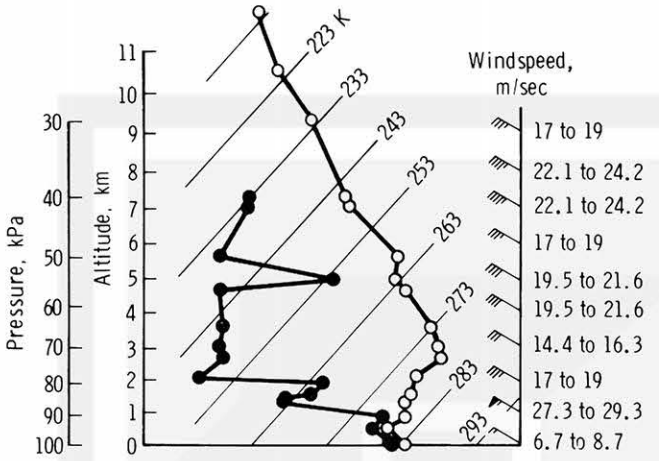

FIGURE 17-18.—Vertical distribution of temperature and wind from Campbell Island at 00:00 GMT, December 16, 1973.

CONCLUSIONS

Examination of mesoscale cloud patterns within the wake of obstacles seen in Skylab photographs reveals the existence of specific types of wake clouds related to meteorological conditions as follows.

1. Cumulus streets occurring when the lapse rate above the surface is adiabatic (a conditionally unstable atmosphere) with a medium to slow flow speed.

2. Kármán vortex streets occurring when the lapse rate above the surface is small, zero, or negative (i.e., a stable atmosphere) with a slow- to medium-speed flow impinging against a relatively large obstacle.

3. Wake waves occurring when the lapse rate above the surface is small (a stable atmosphere) with a medium- to fast-speed flow impinging against a relatively small obstacle. When the flow speed exceeds a critical value, the transverse waves tend to disappear, leaving the diverging waves only.

The human decision in photographing specific phenomena as viewed from a space platform is extremely valuable and important. Skylab photography has demonstrated that new phenomena can be found and photographed efficiently. Such space photography emphasizes the value of human judgment, for which there is no substitute.

REFERENCES

17-1. Briggs, Geoffrey A.; and Leovy, Conway B .: Mariner 9 Observations of the Mars North Polar Hood. Bull. American Meteorol. Soc., vol. 55, no. 4, Apr. 1974, pp. 278-296.

17-2. Chopra, Kuldip P.; and Hubert, Lester F.: Kármán Vortex Streets in Earth's Atmosphere. Nature, vol. 203, no. 4952, Sept. 26, 1964, pp. 1341-1343.

17-3. Chopra, Kuldip P.; and Hubert, Lester F.: Kármán Vortex Streets in Wakes of Islands. J. American Inst. Aeronaut. & Astronaut., vol. 3, no. 10, Oct. 1965, pp. 1941-1943.

17-4. Tsuchiya, K.; and Fujita, T.: A Satellite Meteorological Study of Evaporation and Cloud Formation Over the Western Pacific Under the Influence of the Winter Monsoon. SMRP Research Paper 55, The University of Chicago, 1966.

17-5. Stoker, James Johnston: Water Waves: The Mathematic Theory With Applications. Interscience Publishers (New York), 1957.

17-6. Kelvin, William Thomson: On the Waves Produced by a Single Impulse in Water of any Depth, or in a Dispersive Medium. Proc. Roy. Soc. (London), ser. A, vol. 42, 1887, pp. 80-85.

17-7. Havelock, T. H.: Wave Resistance Theory and its Application to Ship Problems. Society of Naval Architects and Marine Engineers, New York, 1950.